ISSN 1063-7834, Physics of the Solid State, 2008, Vol. 50, No. 9, pp. 1625–1630. © Pleiades Publishing, Ltd., 2008.

PROCEEDINGS OF THE XIII FEOFILOV SYMPOSIUM "SPECTROSCOPY OF CRYSTALS DOPED BY RARE-EARTH AND TRANSITION-METAL IONS"

(Irkutsk, July 9–13, 2007)

VUV $5d$–$4f$ Luminescence of Gd^{3+} and Lu^{3+} Ions in the CaF_2 Host[1]

V. N. Makhov[a, b], S. Kh. Batygov[c], L. N. Dmitruk[c], M. Kirm[b], S. Vielhauer[b], and G. Stryganyuk[d]

[a] *Lebedev Physical Institute, Russian Academy of Sciences, Leninskiĭ pr. 53, Moscow, 119991 Russia*
e-mail: makhov@sci.lebedev.ru

[b] *Institute of Physics, University of Tartu, Tartu, 51014 Estonia*

[c] *General Physics Institute, Russian Academy of Sciences, ul. Vavilova 38, Moscow, 119991 Russia*

[d] *Hamburger Synchrotronstrahlungslabor HASYLAB, Deutsches Elektronensynchrotron DESY, Hamburg, 22607 Germany*

Abstract—The first observation and characterization of Lu^{3+} $4f^{13}5d$–$4f^{14}$ luminescence from the $CaF_2 : Lu^{3+}$ crystal are reported, and the multisite structure in the spectra of Ce^{3+}, Gd^{3+}, and Lu^{3+} ions in the CaF_2 host is analyzed with the high-resolution VUV spectroscopy technique using synchrotron radiation. It is shown that vibronic structure in the emission and excitation spectra of interconfigurational transitions in Gd^{3+} and Lu^{3+} ions doped into CaF_2 differs from that observed for Ce^{3+} ions entering mainly at the tetragonal (C_{4v}) sites. However, the exact types of sites in which the Gd^{3+} and Lu^{3+} ions reside in a CaF_2 lattice cannot be identified using only the obtained experimental spectroscopic data.

PACS numbers: 78.55.Hx, 71.70.Ch, 63.20.Kr, 78.47.+p

DOI: 10.1134/S1063783408090059

1. INTRODUCTION

Trivalent rare-earth (*RE*) ions incorporated into CaF_2 substitute for Ca^{2+} ions. The extra positive charge of the RE^{3+} ion relative to Ca^{2+} needs some mechanism of charge compensation. It is usually accepted that, at a doping concentration below ~0.1%, RE^{3+} ions of any kind reside in CaF_2 predominantly in the tetragonal C_{4v} sites where charge compensation of RE^{3+} is achieved by an interstitial fluorine ion located at the nearest neighbor position along the [100] direction from the RE^{3+} ion [1–3]. The vibronic structure in the spectra of interconfigurational $4f^n$–$4f^{n-1}5d$ transitions in most of the RE^{3+} ions located at the tetragonal sites is dominated by a line at an energy interval of ~480 cm^{-1} from zero-phonon lines (ZPL). However, the RE^{3+} centers of different symmetry have also been detected for many RE^{3+} ions [4–6]. In particular, the trigonal centers (C_{3v}) are observed, in which charge compensation is achieved by a fluorine ion in the next-nearest neighbor position along the [111] direction from the RE^{3+} ion (if crystals were grown under reducing conditions). The cubic (O_h) centers with remote charge compensation by monovalent impurity ions, e.g., by doping with Na^+ or Li^+, have also been identified [7, 8].

Recent studies [9–13] have revealed that several Gd^{3+}- and Lu^{3+}-containing fluoride crystals with a sufficiently wide bandgap emit luminescence in the deep vacuum ultraviolet (VUV) spectral range ($h\nu$ ~ 10 eV), which is due to interconfigurational $4f^6 5d$–$4f^7$ transitions in the Gd^{3+} ion and $4f^{13}5d$–$4f^{14}$ transitions in the Lu^{3+} ion. In crystals with scheelite ($LiYF_4$) or YF_3 structure, the Gd^{3+} and Lu^{3+} ions substitute for Y^{3+} ions almost without distortion of the crystal lattice. As a result, the vibronic structure in the spectra of different RE^{3+} ions looks very similar, being determined by the phonon spectrum of the host lattice. In particular, the fine structure of the Gd^{3+} $4f^6 5d$–$4f^7$ emission spectrum almost coincides in shape with that of the Ce^{3+} $4f$–$5d$ excitation (absorption) spectrum for $LiGdF_4 : Ce^{3+}$ crystal [12]. On the other hand, it was found that the vibronic structure in the emission and excitation spectra of Gd^{3+} $4f^6 5d$–$4f^7$ luminescence from the $CaF_2 : (Gd^{3+}, Ce^{3+})$ crystal [13] differs significantly from that observed for other trivalent *RE* ions doped into CaF_2, similarly to earlier observations in the Gd^{3+} $4f^7$–$4f^6 5d$ absorption spectrum of $CaF_2 : Gd^{3+}$ [14]. In the present work, the Lu^{3+} $4f^{13}5d$–$4f^{14}$ luminescence from the $CaF_2 : (Lu^{3+}, Ce^{3+})$ crystal was detected, assigned, and characterized and the multisite structure in the spectra of Ce^{3+}, Gd^{3+}, and Lu^{3+} ions in the CaF_2 host was analyzed using the high-resolution VUV spectroscopy technique.

[1] The text was submitted by the authors in English.

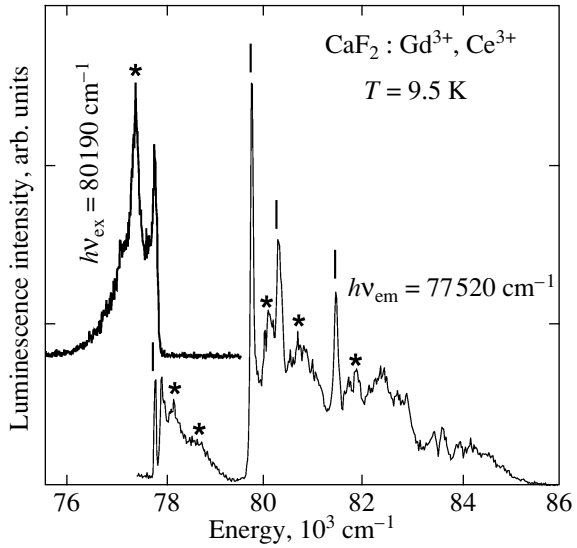

Fig. 1. High-resolution ($\Delta\lambda \sim 1$ Å) VUV emission spectrum under 124.7-nm excitation (bold solid curve) and high-resolution ($\Delta\lambda \sim 1$ Å) excitation spectrum of Gd^{3+} $4f^6 5d$–$4f^7$ emission at 129 nm (thin solid curve) from a $CaF_2 : (Gd^{3+}$ (0.1%), Ce^{3+} (0.05%)) crystal. Spectral lines tentatively ascribed to ZPLs are marked by short lines, and to dominating vibronic lines, by asterisks. $T = 9.5$ K.

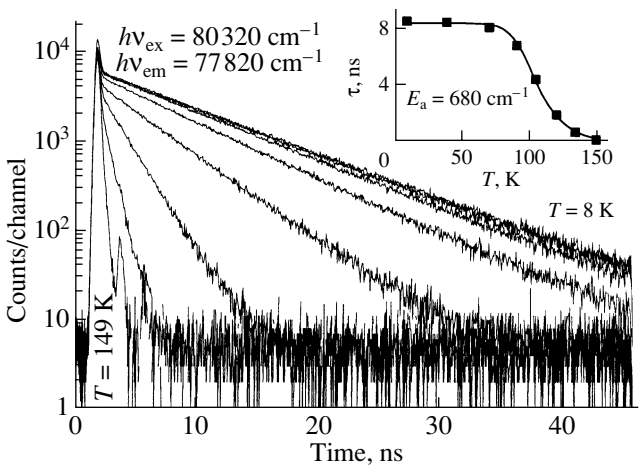

Fig. 2. Temperature dependence of the decay kinetics of Gd^{3+} $4f^6 5d$–$4f^7$ emission from a $CaF_2 : (Gd^{3+}$ (0.1%), Ce^{3+} (0.05%)) crystal measured at 8, 38, 69, 89, 104, 119, 134, and 149 K. The inset shows the temperature dependence of the decay time (see text for details).

2. EXPERIMENTAL DETAILS

High-resolution emission and excitation spectra were measured using the SUPERLUMI setup operated at the DORIS storage ring of HASYLAB at DESY [15, 16]. VUV emission spectra were recorded using an open position-sensitive microchannel-plate detector coated with CsI in combination with a 1-m VUV monochromator, at resolutions better than 0.5 Å in second order. The excitation spectra of VUV emission were recorded using a Pouey-type monochromator (typical spectral resolution $\Delta\lambda = 20$ Å) equipped with a CsI sensitized microsphere plate detector. A 0.3-m Czerny-Turner-type monochromator–spectrograph SpectraPro-308i (Acton Research Inc.) with an R6358P (Hamamatsu) photomultiplier tube was applied for measuring excitation spectra of UV/visible luminescence. Emission spectra in the UV/visible spectral range were recorded on the same SpectraPro-308i spectrograph with a liquid-nitrogen cooled CCD detector (Princeton Instruments Inc.). A spectral resolution of ~0.2 nm was achieved with a 1200-grooves/mm grating using a 0.05-mm slit width. The excitation spectra were recorded with an instrumental resolution of primary monochromator as high as 0.7 Å. The wavelength positions of all features in VUV emission and excitation spectra were determined with an accuracy of ~0.5 Å.

Single crystals of CaF_2 singly doped with 0.1 mol % Ce^{3+}, doubly doped with 0.1 mol % Gd^{3+} and 0.05 mol % Ce^{3+}, and doubly doped with 0.04 mol % Lu^{3+} and 0.02 mol % Ce^{3+} were grown by the vertical Bridgman method in a fluorine atmosphere. The samples were cleaved prior to the mounting onto a copper sample holder attached to the cold finger of a flow-type liquid-helium cryostat (Cryovac GmbH).

3. RESULTS AND DISCUSSION

Fast ($\tau \sim 8.5$ ns) VUV luminescence is observed from the Gd^{3+}-doped CaF_2 crystals, which is due to $4f^6 5d$–$4f^7$ radiative transitions in Gd^{3+} (Fig. 1) [13]. The emission spectrum shows a ZPL at 77760 cm^{-1}, coinciding with the ZPL in the excitation spectrum, and a dominating vibronic line at an energy distance of ~370 cm^{-1}. The excitation spectrum of VUV luminescence agrees well with the Gd^{3+} $4f^7$–$4f^6 5d$ absorption spectrum in $CaF_2 : Gd^{3+}$ obtained in [14]. In addition to the structure above the edge at 77760 cm^{-1}, the excitation spectrum shows a rather rich and well-pronounced structure above ZPL at 79710 cm^{-1}.

VUV luminescence from $CaF_2 : Gd^{3+}$ is observed only at low temperatures and is completely quenched near 150 K. The temperature dependence of the VUV luminescence decay curves is shown in Fig. 2. The decay kinetics are single-exponential at any temperature. The dependence of the decay time on temperature was fitted by a standard formula for thermal quenching via an activation barrier E_a, namely, $\tau = [1/\tau_r + (1/\tau_{nr})\exp(-E_a/k_B T)]^{-1}$ (shown in the inset to Fig. 2), where τ_r is the radiative decay time (8.5 ± 0.1 ns at 10 K) and the second term in this formula describes the temperature dependence of the nonradiative decay. An activation energy $E_a \sim 680$ cm^{-1} for thermal quenching was obtained from the fit. Thermal quenching of $Gd^{3+}5d$–$4f$ luminescence is attributed to phonon-

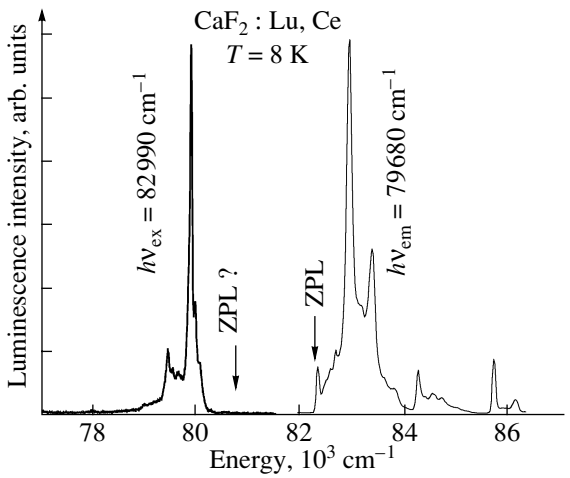

Fig. 3. Lu^{3+} $4f^{13}5d$–$4f^{14}$ emission (bold solid curve) and $4f^{14}$–$4f^{13}5d$ excitation (thin solid curve) spectra from a CaF_2 : (Lu^{3+} (0.04%), Ce^{3+} (0.02%)) crystal at $T = 8$ K.

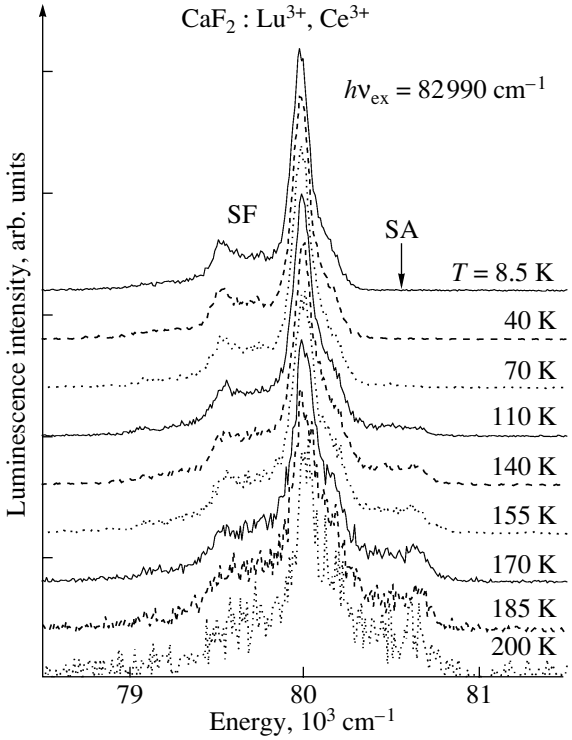

Fig. 4. Normalized emission spectra from a CaF_2 : (Lu^{3+} (0.04%), Ce^{3+} (0.02%)) crystal excited by 120.5-nm photons at various temperatures (measured with moderate resolution).

assisted nonradiative relaxation (intersystem crossing) from the lowest $Gd^{3+}5d$ level to lower-lying $4f$ levels since many $4f$ levels are located in the same energy region as the $5d$ state. The direct $5d$–$4f$ nonradiative transitions (at low temperature) are heavily spin-forbidden because the spin multiplicity of the lowest $4f^6 5d$ level of Gd^{3+} is 8, whereas the $4f^7$ levels of Gd^{3+} closest to the $4f^6 5d$ level are spin doublets or quartets [17].

Only slow VUV luminescence is detected from the Lu^{3+}-doped CaF_2 crystals, with a dominating peak at 79980 cm^{-1} (Figs. 3, 4). This luminescence is ascribed to $4f^{13}5d$–$4f^{14}$ radiative transitions in Lu^{3+}. Similarly to the results obtained in [12] for $LiLuF_4$ and $LiYF_4$: Lu^{3+}, only spin-forbidden (SF) $5d$–$4f$ luminescence of Lu^{3+} is observed from CaF_2 : Lu^{3+} at low temperatures. However, an increase of temperature above 100 K causes the appearance of an additional higher-energy emission band attributed to spin-allowed (SA) $5d$–$4f$ transitions (Fig. 4). The excitation spectra of both bands coincide and correspond to SA $4f^{14}$–$4f^{13}5d$ transitions in Lu^{3+}. From the shape of the emission spectrum at $T >$ 100 K, the splitting between higher-lying low-spin (LS) ($S = 0$) and lower-lying high-spin (HS) ($S = 1$) $4f^{13}5d$ levels of Lu^{3+} in CaF_2, from which SA and SF $5d$–$4f$ transitions take place, respectively, can be estimated to be less than two phonon energies. As a result, the rate of phonon-assisted nonradiative relaxation considerably exceeds that of the radiative decay for the higher-lying LS $4f^{13}5d$ state of Lu^{3+}; so, at a low temperature, only SF $5d$–$4f$ luminescence from Lu^{3+} is observed. An increase in temperature opens another decay channel for the lowest HS $4f^{13}5d$ state of Lu^{3+}, namely, the thermal population of the higher-lying LS $4f^{13}5d$ state, from which the $5d$–$4f$ radiative transitions are spin-allowed. However, because of the "indirect" thermal mechanism of population, the decay kinetics of SA luminescence are controlled by the slow decay of SF transitions.

At a low temperature, the spectrum of VUV luminescence from CaF_2 : Lu^{3+} shows no ZPL (similarly to the case of $LiYF_4$: Lu^{3+} [12]) because purely electronic SF $4f^{13}5d$–$4f^{14}$ transitions in Lu^{3+} are very weak (Fig. 3). The narrow lines observed in the spectrum are due to vibronic states. The excitation spectrum of this emission shows ZPL at 82 420 cm^{-1}, which should correspond to the edge of SA $4f^{14}$–$4f^{13}5d$ transitions in Lu^{3+}. The presence of a distinct vibronic structure in the spectra clearly shows that electron–lattice coupling between the $4f^{13}5d$ electronic configuration of the Lu^{3+} ion and the lattice vibrations in CaF_2 : Lu^{3+} is rather weak and the Stokes shift between emission and absorption cannot be large.

However, there is a "Stokes shift" of ~1750 cm^{-1} between experimental emission and excitation spectra obtained at $T >$ 100 K for Lu^{3+} SA $4f$–$5d$ transitions. This fact can be explained, in principle, if one assumes that emission occurs from Lu^{3+} ions occupying sites (available in smaller concentration) that differ from those responsible for $4f$–$5d$ absorption (available in larger concentration). However, for such small concentrations of Lu^{3+} as ~0.04 mol %, efficient energy trans-

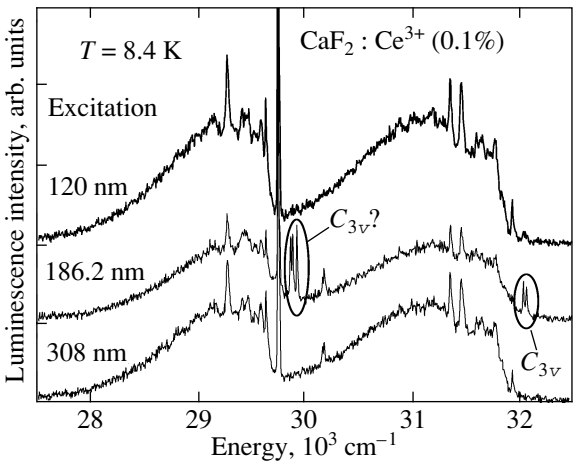

Fig. 5. Ce^{3+} 5*d*–4*f* emission spectrum measured from a $CaF_2 : Ce^{3+}$ (0.1 mol %) crystal under excitation to the lowest and higher-lying Ce^{3+} 5*d* bands. $T = 8.4$ K. The features assigned to ZPLs of 5*d*–4*f* transitions in Ce^{3+} ions occupying trigonal (C_{3v}) sites are marked.

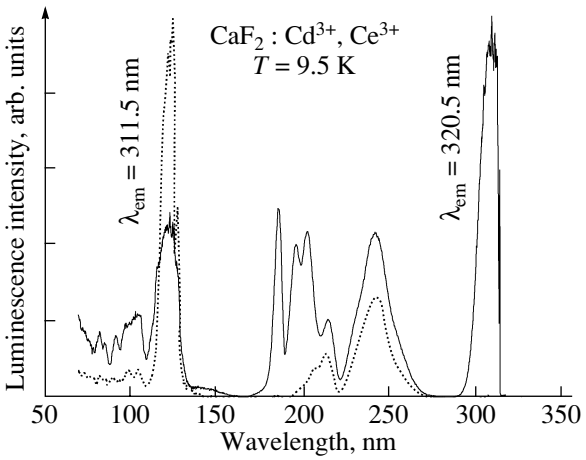

Fig. 6. Excitation spectra of Gd^{3+} $^6P_{7/2}$–$^8S_{7/2}$ emission at 311.5 nm (dotted curve) and of Ce^{3+} 5*d*–4*f* emission at 320.5 nm (solid curve) from a CaF_2 : (Gd^{3+} (0.1%), Ce^{3+} (0.05%)) crystal. $T = 9.5$ K.

fer between different types of Lu^{3+} centers cannot be expected. On the other hand, theoretical calculations performed for 4*f*–5*d* absorption of Lu^{3+} introduced into $LiYF_4$ (local symmetry S_4) have shown that the absorption coefficient for the bands at the edge of Lu^{3+} 4*f*–5*d* SA transitions is much smaller (by more than an order of magnitude) than that in the region situated at ~1400 cm^{-1} above the edge [12]. For such small doping concentrations of Lu^{3+} as 0.04 mol %, the lowest energy bands can be very weak and not seen in the experimental spectra. Following the approach developed in [18] for predicting the energy of the lowest 5*d* level of RE^{3+} in a particular host and taking into account that the energy of ZPL for the lowest 4*f*–5*d* transition of Ce^{3+} in CaF_2 is 31 930 cm^{-1} (Fig. 5), the energy of the lowest Lu^{3+} LS ($S = 0$) $4f^{13}5d$ level in $CaF_2 : Lu^{3+}$ is expected to be ~81 100 cm^{-1}, which is much smaller than the energy of ZPL in the excitation spectrum and is much larger than the energy of the high-energy SA band in the VUV emission spectrum of $CaF_2 : Lu^{3+}$. So, additional experimental and theoretical studies are needed to find out the nature of the observed unusual "Stokes shift."

The Lu^{3+} 5*d*–4*f* luminescence is almost completely quenched at temperatures $T > 200$ K. The Lu^{3+} ion has no excited 4*f* levels, and therefore thermal quenching of Lu^{3+} 5*d*–4*f* luminescence cannot be due to nonradiative transitions to 4*f* levels and should be attributed to thermally activated ionization of 5*d* electrons to the conduction band. Taking into account that the energy separation between the lowest 5*d* (HS) level and the bottom of the conduction band is the smallest for Lu^{3+} among all *RE* ions [19], it can be expected that the 5*d*–4*f* luminescence from Lu^{3+} is quenched at lower temperatures than that from Er^{3+} or Tm^{3+} ($T > 500$ K [20]).

The lowest energy band in the Ce^{3+} 4*f*–5*d* excitation spectrum and the Ce^{3+} 5*d*–4*f* emission spectrum measured under excitation into this lowest energy excitation band correspond well to the spectra of the Ce^{3+} center in CaF_2 in a tetragonal (C_{4v}) site [1–3] for all singly and doubly doped CaF_2 samples studied here (Figs. 5 and 6). As expected, the vibronic structure in these spectra is dominated by the line at an energy interval ~480 cm^{-1} from the ZPL, which corresponds well to the longitudinal optical phonon energy in CaF_2 [21], but has been usually interpreted as the local breathing oscillation mode of the eight fluorine ions surrounding the Ce^{3+} ion [22]. The excitation spectra of Ce^{3+} 5*d*–4*f* emission are also very similar for all three kinds of Ce^{3+}-containing samples. In addition to the excitation band corresponding to transitions to the lowest Ce^{3+} 5*d* level (originating from the E_g band of cubic symmetry), a group of three bands in the range 180–205 nm is observed in the spectrum, which correspond to transitions to the Ce^{3+} 5*d* states in a site of C_{4v} symmetry originating from the T_{2g} band of cubic symmetry [2]. The bands at ~240 and ~214 nm, also observed in the spectra of all samples studied, should belong to another kind of Ce^{3+} centers and are usually explained as being due to absorption by Ce^{3+} clusters.

As was shown in [2], the absorption spectrum of trigonal (C_{3v}) Ce^{3+} centers has a specific feature at the edge of the 4*f*–5*d* absorption, namely, two closely spaced lines (separated by ~30 cm^{-1}) corresponding to absorption from the ground 4*f* level and from the first excited 4*f* level of the $^2F_{5/2}$ ground multiplet. The latter

"hot line" appears in the absorption spectrum at a high enough temperature and is very weak at 15 K. However, in the emission spectrum, both the lines should be well seen at a low temperature as well. Indeed, a characteristic double-line feature can be clearly observed in the Ce^{3+} 5*d*–4*f* emission spectra measured from all three types of Ce^{3+}-doped crystals under excitation to higher-lying rather than to the lowest 5*d* band (Fig. 5). The energy difference (~135 cm^{-1}) between the shortest wavelength line in this doublet and the ZPL in the spectrum of Ce^{3+} 5*d*–4*f* emission from tetragonal (C_{4v}) centers should be considered as the energy difference between the lowest 5*d* levels of Ce^{3+} ions occupying tetragonal (C_{4v}) and trigonal (C_{3v}) sites. The 4*f*–5*d* excitation bands of Ce^{3+} in C_{3v} sites are hidden behind the intense 4*f*–5*d* excitation bands of Ce^{3+} in C_{4v} sites since the concentration of the latter centers is obviously much higher.

Simultaneously with the doublet feature on the short-wavelength side of the emission spectrum, another feature consisting of three lines appears on the short-wavelength side of the ZPL corresponding to Ce^{3+} 5*d*–4*f* ($^2F_{7/2}$) transitions in tetragonal (C_{4v}) centers (Fig. 5). These three lines should be assigned to transitions from the lowest 5*d* level to the lowest and two excited Stark levels of the 4*f* ($^2F_{7/2}$) multiplet of Ce^{3+} in the trigonal (C_{3v}) sites. Taking into account the 135-cm^{-1} difference between the lowest 5*d* levels of Ce^{3+} ions in tetragonal (C_{4v}) and trigonal (C_{3v}) sites, we find that the lowest level of the 4*f* ($^2F_{7/2}$) multiplet should have a lower energy (by ~45 cm^{-1}) for the trigonal (C_{3v}) site than for the tetragonal (C_{4v}) site.

As is clearly seen in Fig. 6, Gd^{3+} $^6P_{7/2}$–$^6S_{7/2}$ emission at ~311 nm is not excited in the CaF_2 : (Gd^{3+}, Ce^{3+}) crystal under excitation to the lowest energy Ce^{3+} 5*d* band, as well as to the group of three bands in the range 180–205 nm, all corresponding to transitions to the Ce^{3+} 5*d* levels in a tetragonal (C_{4v}) site. Thus, absorption of a photon by the Ce^{3+} ion in a tetragonal site results in fast energy relaxation to the lowest Ce^{3+} 5*d* level from which the characteristic Ce^{3+} 5*d*–4*f* emission is observed. No energy transfer to Gd^{3+} is observed in this case because the energy of the lowest 5*d* level of Ce^{3+} in a tetragonal site is lower than that of the Gd^{3+} 4*f* ($^6P_{7/2}$) level. The Gd^{3+} 311-nm emission is well excited in the region of the 240- and 213-nm excitation bands, which are assigned to 4*f*–5*d* transitions in Ce^{3+} clusters. This occurs because the energy of the lowest 5*d* level of Ce^{3+} in such centers is higher than or nearly the same as the energy of the Gd^{3+} 4*f* ($^6P_{7/2}$) level. Accordingly, energy transfer can take place from these Ce^{3+} centers to Gd^{3+}.

Although theoretical calculations of interconfigurational transitions in Gd^{3+} and Lu^{3+} ions doped into CaF_2 are not available, some narrow lines in the spectra can be tentatively ascribed to ZPLs accompanied by a vibronic structure. Such a simplified analysis allows anyway to make a conclusion that the fine structure in the emission and excitation spectra of interconfigurational transitions in these ions is definitely not dominated by the vibronic lines at an energy interval of ~480 cm^{-1} from ZPLs. This indicates that Gd^{3+} and Lu^{3+} ions reside in CaF_2 predominantly in sites differing from tetragonal (C_{4v}) sites. The main features of the vibronic structure in the Gd^{3+} $4f^6 5d$–$4f^7$ emission spectrum and in the lowest energy band of the Gd^{3+} $4f^7$–$4f^6 5d$ excitation spectrum are separated by ~370 cm^{-1} from ZPLs. This energy does not correspond to any well-defined peak in the phonon spectrum of CaF_2, and some pseudo-local modes should be involved in the electron–lattice coupling between the $4f^6 5d$ electronic configuration of the Gd^{3+} ion and the lattice vibrations in CaF_2. An analysis of the vibronic structure in the spectra of interconfigurational transitions in Lu^{3+} is even more complicated since ZPL is not observed in the spectrum of Lu^{3+} SF $4f^{13}5d$–$4f^{14}$ luminescence.

4. CONCLUSIONS

By using the high-resolution VUV spectroscopy technique, the Lu^{3+} $4f^{13}5d$–$4f^{14}$ luminescence from the CaF_2 : (Lu^{3+}, Ce^{3+}) crystal has been detected, assigned, and characterized. The measurements of emission spectra under spectrally selective excitation from CaF_2 doubly doped with Gd^{3+} and Ce^{3+} or Lu^{3+} and Ce^{3+}, as well as singly doped with Ce^{3+}, have confirmed that, for doping concentrations below ~0.1 mol %, the Ce^{3+} ions reside in CaF_2 predominantly in the tetragonal (C_{4v}) sites. However, the presence of trigonal (C_{3v}) Ce^{3+} centers was also detected and several lines in the emission spectra were assigned to ZPLs corresponding to 5*d*–4*f* transitions in Ce^{3+} entering the trigonal (C_{3v}) sites. The vibronic structure in the emission and excitation spectra of interconfigurational transitions in Gd^{3+} and Lu^{3+} ions in CaF_2 differs from that observed for Ce^{3+} ions at the tetragonal (C_{4v}) sites. However, the types of sites in which the Gd^{3+} and Lu^{3+} ions reside in the CaF_2 lattice cannot be identified using only the experimental spectroscopic data available.

ACKNOWLEDGMENTS

The authors would like to thank Prof. G. Zimmerer and Prof. B.Z. Malkin for valuable discussions.

This work was supported by the RFBR (project no. 05-02-1730), the Estonian Science Foundation (grant no. 6538), and the European Community Research Infrastructure Action within the FP6 Program through the Contract RII3-CT-2004-506008 (IA-SFS).

REFERENCES

1. A. A. Kaplyanskiĭ, V. N. Medvedev, and P. P. Feofilov, Opt. Spektrosk. **14**, 644 (1963).
2. W. J. Manthey, Phys. Rev. B: Solid State **8**, 4086 (1973).
3. T. Szczurek and M. Schlesinger, in *Rare-Earth Spectroscopy*, Ed. by B. Jezowska-Trebiatowska, J. Legendziewich, and W. Strek (World Sci., Singapore, 1985), p. 309.
4. Y. K. Voron'ko, A. A. Kaminski, and V. V. Osiko, Zh. Éksp. Teor. Fiz. **50** (1), 15 (1966) [Sov. Phys. JETP **23** (1), 10 (1966)].
5. I. T. Jacobs, G. D. Jones, K. Zdansky, and R. A. Satten, Phys. Rev. B: Solid State **3**, 2888 (1971).
6. M. Yamaga, S. Yabashi, Y. Masui, M. Honda, H. Takahashi, M. Sakai, N. Sarukura. J.-P. R. Wells, and G. D. Jones, J. Lumin. **108**, 307 (2004).
7. P. W. Pack, W. J. Manthey, and D. S. McClure, Phys. Rev. B: Condens. Matter **40**, 9930 (1989).
8. S. P. Jamison, R. J. Reeves, P. P. Pavlichuk, and G. D. Jones, J. Lumin. **83–84**, 429 (1999).
9. M. Kirm, J. C. Krupa, V. N. Makhov, M. True, S. Vielhauer, and G. Zimmerer, Phys. Rev. B: Condens. Matter **70**, 241 101(R) (2004).
10. M. Kirm, V. N. Makhov, M. True, S. Vielhauer, and G. Zimmerer, Fiz. Tverd. Tela (St. Petersburg) **47** (8), 1368 (2005) [Phys. Solid State **47** (8), 1416 (2005)].
11. V. N. Makhov, J. C. Krupa, M. Kirm, G. Stryganyuk, S. Vielhauer, and G. Zimmerer, Izv. Vyssh. Uchebn. Zaved., Fiz., No. 4 (Suppl.), 86 (2006).
12. M. Kirm, G. Stryganyuk, S. Vielhauer, G. Zimmerer, V. N. Makhov, B. Z. Malkin, O. V. Solovyev, R. Yu. Abdulsabirov, and S. L. Korableva, Phys. Rev. B: Condens. Matter **75**, 075 111 (2007).
13. V. N. Makhov, S. Kh. Batygov, L. N. Dmitruk, M. Kirm, G. Stryganyuk, and G. G. Zimmerer, Phys. Status. Solidi C **4**, 881 (2007).
14. M. Schlesinger, T. Szczurek, and G. W. F. Drake, Solid State Commun. **28**, 165 (1978).
15. G. Zimmerer, Nucl. Instrum. Methods Phys. Res., Sect. A **308**, 178 (1991).
16. G. Zimmerer, Radiat. Meas. **42**, 859 (2007).
17. P. S. Peijzel, A. Meijerink, R. T. Wegh, M. F. Reid, and G. W. Burdick, J. Solid State Chem. **178**, 448 (2005).
18. P. Dorenbos, J. Lumin. **91**, 91 (2000).
19. P. Dorenbos, J. Phys.: Condens. Matter **15**, 8417 (2003).
20. V. N. Makhov, T. Adamberg, M. Kirm, S. Vielhauer, and G. Stryganyuk, J. Lumin. **128**, 725 (2008).
21. R. P. Lowndes, J. Phys. C: Solid State Phys. **4**, 3083 (1971).
22. W. Hayes, M. C. K. Wiltshire, W. J. Manthey, and D. S. McClure, J. Phys. C: Solid State Phys. **6**, L273 (1973).